DNA-Templated Assemblies of Nickel Hexacyanoferrate Crystals

Nitin Bagkar,*,†,‡ Sipra Choudhury,† Shovit Bhattacharya,§ and Jatinder V. Yakhmi*,§

Chemistry Division and Technical Physics and Prototype Engineering Division, Bhabha Atomic Research Centre, Mumbai 400 085, India

Received: December 7, 2007; Revised Manuscript Received: February 28, 2008

We report here the synthesis of nickel hexacyanoferrate (NiHCF) crystals using calf thymus DNA (CT-DNA) as a template. The double-stranded CT-DNA has been used as a template to self-assemble NiHCF crystals and to produce aggregates having different morphologies at different temperatures. The guided self-assembly behavior of DNA was studied at different temperatures by scanning electron microscopy. The cube-shaped crystals of NiHCF with an average diameter of 400 nm are observed along the DNA framework at room temperature; however, at higher temperatures, the morphology of NiHCF changed from open tubular to dendrimer. The intermediate temperatures show long chains (up to many micrometers) and spherical structures of NiHCF crystals. The micrometer long DNA template plays a key role in the formation of extended arrays of NiHCF crystals, suggesting that the templating action is retained even at the higher temperatures.

1. Introduction

The organization of magnetic, metallic, or semiconducting crystals by self-assembly from molecular building blocks continues to inspire novel strategies for the fabrication of functional nanostructured materials. Biological macromolecules, such as proteins and nucleic acids, have also been used extensively for the organization of nanostructured materials. Among them, DNA offers a great potential as a building block, because of its unique molecular recognition and mechanical and self-assembling characteristics[1–3] and has, therefore, even been used to construct nanomechanical devices[4,5] and molecular computing systems.[6,7] Naturally occurring DNA has a linear helical structure consisting of two chains, each with a backbone of phosphate and sugar molecules. Upon heating, the DNA base pair opens up because of denaturation, and subsequent random aggregation results in beautiful fractal structures; these morphological changes, related to the melting behavior of DNA, have been well-studied.[8] Controlled self-assembly of cross-linked metal nanoparticles utilizing the templating action of DNA has also been reported at room temperature (RT)[9–12] including the use of denatured herring sperm DNA as a template for the self-assembly of magnetic nanowire assemblies, with potential for low-field magnetic resonance imaging applications.[13] However, there are no detailed reports on the elucidation of morphological changes of functional nanomaterials accompanying the templating action of DNA, triggered by its denaturation, at intermediate and higher temperatures.

The objective of the present investigation is to study the influence of DNA on the self-assembly behavior of magnetic nanoparticles at different temperatures. We have used nickel hexacyanoferrate $\{Ni_3[Fe(CN)_6]_2 \cdot 14H_2O\}$,[14] nicknamed NiHCF, belonging to the Prussian blue family of magnetic compounds, known for the tunability of their magnetic properties, through the substitution of transition metals in the carbon and nitrogen coordination of the bridging cyanide ligand.[15,16] In the process, we have discovered a novel method to grow the crystals of NiHCF, using double-stranded calf thymus DNA (CT-DNA) as a template. These crystals can be arranged in linear and nonlinear multibranched morphologies of the template, depending on the temperature treatment. This happens because of the denaturation of DNA, which occurs above its melting temperature (about 80 °C), although the actual process starts much below this temperature.[8] The denaturation process is accompanied by breaking of hydrogen bonds with concomitant changes in the morphology of DNA. The double-stranded DNA gets separated into single strands upon thermal agitation, and DNA undergoes subsequent morphological changes from open circular to globular structures. The globular structure is indicative of complete denaturation of DNA. On heating up to still higher temperatures, the globular structure transforms into beautiful fractal structures due to diffusion-limited aggregation of small clusters.[17–21] Thus, as a function of temperature, the NiHCF crystals self-assemble into linear ropes, spheres, and dendritic structures.

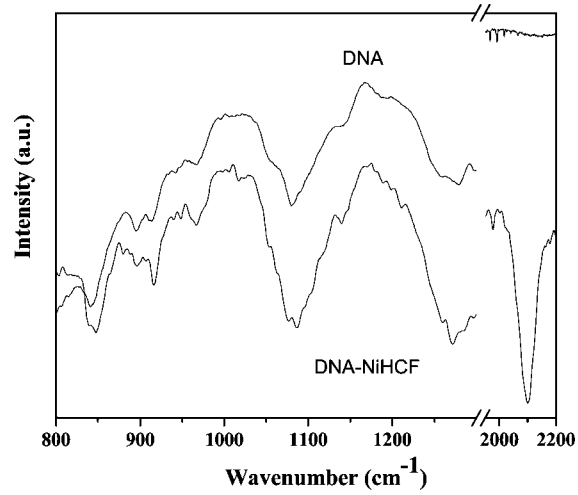

Figure 1. FTIR spectra of DNA and DNA−NiHCF conjugate in solution at RT.

* To whom correspondence should be addressed. E-mail: (N.B.) nitin_b10@yahoo.com or (J.V.Y.) yakhmi@barc.gov.in.

† Chemistry Division.

‡ Present address: Department of Chemistry, National Taiwan University, Taiwan 106, Taiwan.

§ Technical Physics and Prototype Engineering Division.

10.1021/jp711536r CCC: $40.75
Published on Web 04/24/2008

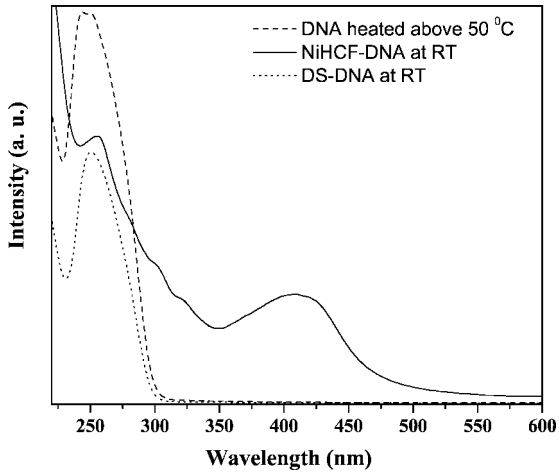

Figure 2. UV–vis spectra of CT-DNA, NiHCF−DNA conjugate at RT, and CT-DNA heated above 50 °C.

2. Experimental Details

2.1. Synthesis. NiHCF is synthesized usually by adding nickel chloride to a solution of potassium hexacyanoferrate in a 3:2 molar ratio.[22] However, in the present work, DNA is incorporated in the synthesis step, and the electrostatic interaction between the DNA and the reactants not only grows the NiHCF crystals at RT but also induces the spontaneous arrangement of these NiHCF crystals along the chains of base pairs. In a typical procedure, a CT-DNA (5 g/mL) was dissolved in triply distilled water so as to make a final concentration of 1 g/mL. To this was added 10 mM potassium ferrocyanide, and the resulting solution was mixed thoroughly in a vortex mixer. An aqueous solution of 10 mM nickel chloride was added to the above solution in a 3:2 ratio. After it was stirred, the solution was kept standing for 1 h. The NiHCF crystals obtained thus were isolated in the solid phase by evaporation and resuspended in water. For SEM characterization, a drop of DNA−NiHCF crystals was spread on a silicon wafer and heated in an oven at 50, 55, 60, 75, and 100 °C for 1 h and used. It must be noted that DNA has a definite role in not only the self-assembly of NiHCF crystals in various morphologies as a function of temperature, details of which are provided later, but also the growth of these crystals; because a control experiment was done without incorporation of DNA, no crystals formed and we obtained only a precipitate of NiHCF.

2.2. Structural Characterization. Fourier-transformed infrared (FTIR) spectra of liquid samples of DNA and NiHCF−DNA conjugate were recorded using a Bomem-MB102 Fourier transform infrared spectrometer. The liquid sample was squeezed between two CaF_2 windows, and the scans were averaged at a resolution of 1 cm^{-1} in the range of 800−3500 cm^{-1}. Optical absorption measurements were carried out on a Chemito Spectrascan UV2600 spectrophotometer (UV–vis) in the wavelength range of 200–600 nm. Scanning electron microscopy (SEM) was carried out by using Digital Microscopy Imaging, Tescan VEGA (VEGA MV2300T).

3. Results and Discussion

Figure 1 shows FTIR spectra of DNA−NiHCF conjugate and pure DNA recorded in the liquid state at the RT. The comparison of FTIR spectra in the 800−1200 cm^{-1} region was helpful in the understanding of the interaction between DNA and nanoparticles. The structurally sensitive FTIR bands give the conformational changes of nucleic bases due to the interaction of DNA with nanoparticles. Both of the samples showed intense absorption in the range of 1050−1100 cm^{-1}

Figure 3. SEM image of DNA−NiHCF conjugate at RT (scale bar, 100 μm). The inset shows uniform distribution of NiHCF crystals over a large area (scale bar, 200 μm).

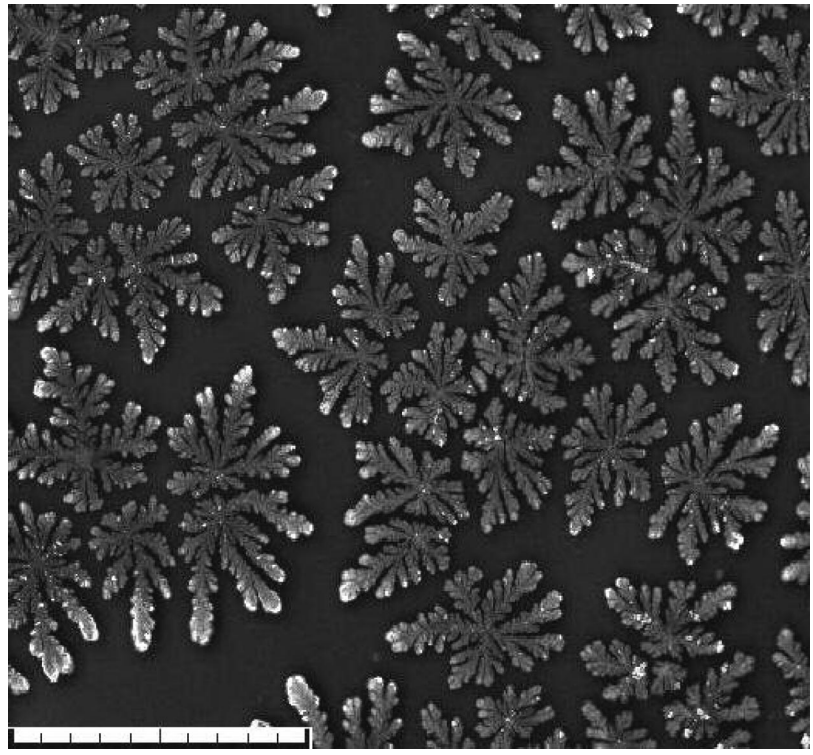

Figure 4. SEM image of dendrites of DNA−NiHCF conjugates at 75 °C (scale bar, 100 μm).

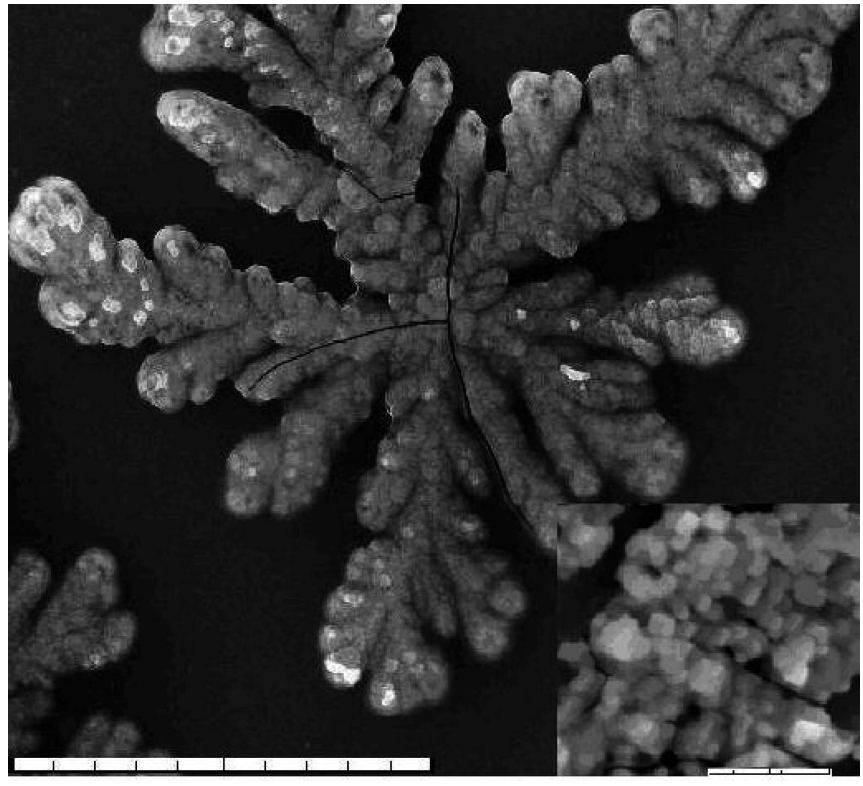

Figure 5. Enlarged view of the arrangement of cubic crystals within dendritic architecture (scale bar, 50 μm). The inset (scale bar, 5 μm) shows the cube-shaped NiHCF crystals.

due to a band from the DNA. The FTIR spectrum of NiHCF−DNA was completely dominated by the features due to DNA. FTIR spectra of pure CT-DNA in liquid state alone showed a peak at 1079 cm^{-1} due to the symmetric stretching mode of the phosphate group ($\nu_s PO^{2-}$), which shifted upward by 6 cm^{-1} (1085 cm^{-1}) in the case of DNA−NiHCF conjugate, indicating the interaction of nanoparticles with the phosphate backbone of DNA.[23] The intensity of the symmetric stretching mode of the PO^{2-} vibrational band was found to depend on the ions in the surroundings of the phosphate groups. The upshift was a consequence of charge neutralization of peripheral charges of the phosphate group by NiHCF, causing strengthening of the PO^{2-} bonds. This clearly indicates that the nanoparticles bind to the DNA

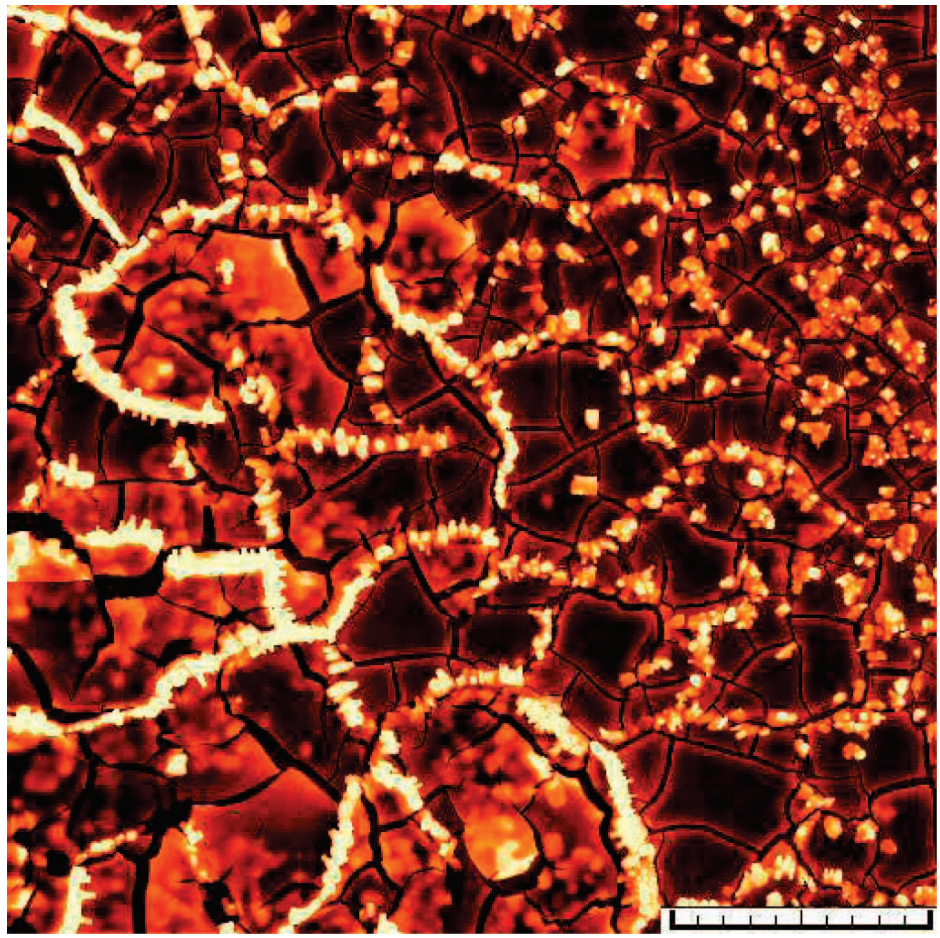

Figure 6. SEM image of DNA−NiHCF conjugate at 50 °C (scale bar, 50 μm).

through negatively charged phosphate ions. The intensity of this band conjugate was also increased for DNA−NiHCF conjugate, indicating the evidence of interaction, which results in the significant enlargement of this band. Thus, from the differences in the intensity and position of characteristic IR bands, conclusions can be drawn about the interaction of DNA and NiHCF in the solution. A new peak emerged at 2167 cm^{-1} for the DNA−NiHCF conjugate, which corresponds to the bridging cyanide (Ni−CN−Fe) cyanide groups, which was not present in the IR spectra of pure CT-DNA.[24] RT UV–vis spectra of CT-DNA, DNA−NiHCF conjugate, and CT-DNA heated above 50 °C are shown in Figure 2. UV–vis spectra for both DNA and DNA−NiHCF conjugate showed the presence of a nucleotide absorbance band at 260 nm, consistent with the spectra for double-stranded CT-DNA. The evidence for DNA and nanoparticle assembly was obtained by monitoring bands at 260 and 410 nm when the suspensions were heated above 50 °C. The increased intensity of the band at 260 nm for DNA−NiHCF conjugate at higher temperature indicated the breaking of double stands into single strands. The band at 410 nm was due to the charge transfer band of NiHCF, which was found absent in the spectrum recorded for CT-DNA. This band did not show any wavelength shift upon heating, which is consistent with the SEM analysis at different temperatures.

To understand the role of DNA in the self-assembly of NiHCF crystals in different morphologies, as one warms them up toward the denaturation temperature of DNA, the DNA-stabilized NiHCF crystals in solution were spread on a silicon substrate and heated at different temperatures and characterized by SEM. Figure 3 shows the SEM image of NiHCF−DNA conjugate at RT, which showed cube-shaped crystals of NiHCF having an average diameter of 400 nm, arranged along the DNA strand framework. The NiHCF crystal assemblies extend along the chain up to lengths of a few micrometers. The NiHCF nanocrystals form aggregates at definite intervals, distributed over the entire length of the strands. The distribution of crystals is uniform over a large area, as shown in the inset of Figure 3 at lower magnification. The energy despersive X-ray (EDX) analysis of the various NiHCF crystallites during SEM analysis showed that the ratio of Ni and Fe was almost 3:2, confirming the composition of NiHCF.

The SEM of DNA−NiHCF conjugates heated at 75 °C is shown in Figure 4. The morphology has changed from an open-chain structure to a fractal (dendritic) structure. The dendritic architecture forms possibly due to nonequilibrium growth of DNA chains[8] and consists of a central core (arising from aggregation of numerous chains) and branching tails emanating from this core. Each lobe of a dendrite is about 10 μm in size. The NiHCF particles within these aggregates retain their physical shape and size, as before heating, which indicates the stabilizing influence that the oligonucleotide has on NiHCF crystals even at higher temperatures. The surface of the dendrimer curls with numerous chain ends, which appears to act as a template, directing the self-assembly of NiHCF crystals along the branching unit. Figure 5 depicts the enlarged view of the assembly of crystals of NiHCF formed by aggregation for one of such branching units. The inset shows the cube-shaped crystals of NiHCF. It is tempting to suggest that our results

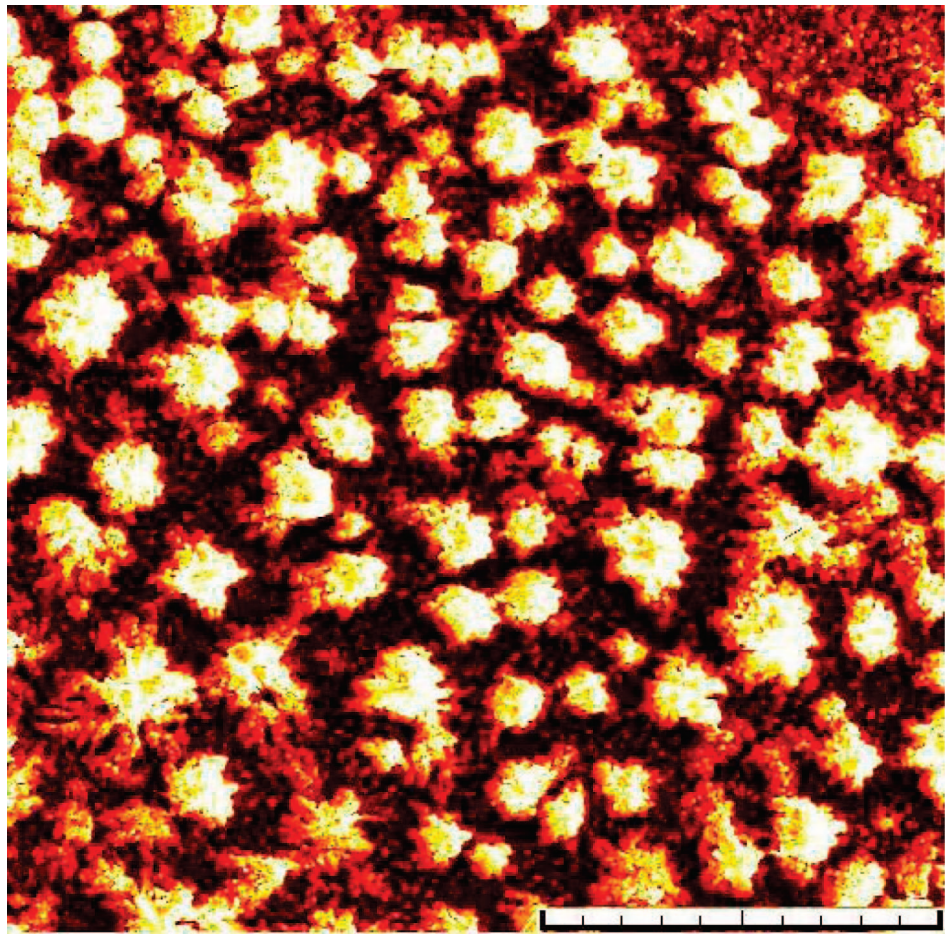

Figure 7. SEM image of spherical globules of DNA−NiHCF at 60 °C (scale bar, 200 μm).

open the doors to the possibility of growth of self-assembled dendritic aggregates of crystals of other classes of functional materials using DNA as a template.

In the literature, the evolution of dendritic structures and the related aggregation process has been analyzed by different models such as the diffusion-limited aggregation (DLA)[25] or cluster–cluster aggregation (CCA).[26,27] In the case of DNA dendrites, the aggregation process occurs as a result of random walk-related DLA, which involves cluster formation by the adhesion of a particle with random walk to a selected seed on contact.[17–21] The process can be elucidated experimentally by using techniques such as acoustic absorption, viscosity, light scattering, etc. To gain insight into the process of the formation of fractals of DNA aggregates in the present case, the NiHCF−DNA solution was heated at intermediate temperatures of 50, 55, and 60 °C, and SEM images of NiHCF−DNA crystals were recorded in each case. Upon heating from RT to 50 °C, the double-stranded DNA breaks up into single strands and a pattern resembling a two-dimensional necklace of NiHCF crystals emerged (Figure 6). These single strands of DNA are aligned in an end-to-end fashion, forming long (up to many micrometers), linear chains of NiHCF crystals. The cube-shaped NiHCF crystals are arranged as linear chains, which are joined in the form of a net, guided by DNA strands.

The DNA denaturation starts at about 55 °C, above which the long chain network structure breaks down into spherical globules due to the disintegration of long chain nucleotide sequences into smaller fragments, subsequent aggregation of which produces spherical globules. On further heating at 60 °C (or higher), the spherical globules start walking randomly because of the thermal motion and therefore diffuse around and stick to the aggregate (core) whenever they come in contact with it. Figure 7 depicts the spherical globular assemblies of NiHCF−DNA conjugates, with a typical diameter of ~10 μm, formed through aggregation of smaller units into NiHCF crystal assemblies of spherical shape, guided by the DNA template. Consequent upon heating, tails of branches start emanating from the sides of a globule in the shape of arms of a fractal structure. This is a significant step toward building up of a dendritic architecture. However, an increase in the temperature above 80 °C causes the disintegration of the fractal structure resulting in the random arrangement of NiHCF crystals. Thus, by temperature programming, one can very well control the assemblies of functional nanomaterials.

4. Conclusions

In summary, the double-stranded CT-DNA has been used as a template to self-assemble NiHCF crystals and to produce aggregates of different morphologies at higher temperatures. The micrometer long DNA template plays a key role in the formation of extended arrays of NiHCF crystals, suggesting that the templating action is retained even at higher temperatures. However, above 75 °C, DNA loses its templating action, resulting in the random arrangement of NiHCF crystals. Our study demonstrates a simple method in which one can control the morphologies of DNA−NiHCF conjugates by temperature programming. Temperature dependence of the DNA self-assembly process can be used for the design and fabrication of complex architectures of functional nanomaterials. The observa-

tions presented here are only a step toward understanding the processing of DNA dendrites in nanotechnology.

Acknowledgment. We thank Dr. Amit Kulkarni for providing CT-DNA samples and Dr. P. A. Hassan for fruitful discussions.

References and Notes

(1) Niemeyer, C. M. *Angew. Chem., Int. Ed. Engl.* **1997**, *36*, 585.
(2) Warner, M. G.; Hutchison, J. E. *Nat. Mater.* **2003**, *2*, 272.
(3) Nam, J.-M.; Park, S.-J.; Mirkin, C. A. *J. Am. Chem. Soc.* **2002**, *124*, 3820.
(4) Mao, C.; Sun, W.; Shen, Z.; Seeman, N. C. *Nature* **1999**, *397*, 144.
(5) Yan, H.; Zhang, X.; Shen, Z; Seeman, N. C. *Nature* **2002**, *415*, 62.
(6) Di-Mauro, E.; Hollenberg, C. P. *Adv. Mater.* **1993**, *5*, 384.
(7) Adleman, L. M. *Science* **1994**, *266*, 1021.
(8) Yan, L.; Iwasaki, H. *Chaos, Solitons Fractals* **2004**, *20*, 877.
(9) Mirkin, C. A.; Letsinger, R. L.; Mucic, R. C.; Storhoff, J. J. *Nature* **1996**, *382*, 607.
(10) Alivisatos, A. P.; Johnson, K.; Peng, X.; Wilson, T. E.; Loweth, C. J.; Bruchez, M.; Schultz, P. G. *Nature* **1996**, *382*, 609.
(11) Storhoff, J. J.; Elghanian, R.; Mucic, R. C.; Mirkin, C. A.; Letsinger, R. L. *J. Am. Chem. Soc.* **1998**, *120*, 1959.
(12) Dujardin, E.; Hsin, L.-B.; Wang, C. R. C.; Mann, S. *Chem. Comm.* **2001**, 1264.
(13) Byrne, S. J.; Corr, S. A.; Gun'ko, Y. K.; Kelly, J. M.; Brougham, D. F.; Ghosh, S. *Chem. Commun.* **2004**, 2560.
(14) Bagkar, N.; Ganguly, R.; Choudhury, S.; Hassan, P. A.; Sawant, S.; Yakhmi, J. V. *J. Mater. Chem.* **2004**, *14*, 1430.
(15) Widmann, A.; Kahlert, H.; Petrovic-Prelevic, I.; Wulff, H.; Yakhmi, J. V.; Bagkar, N.; Scholz, F. *Inorg. Chem.* **2002**, *41*, 5706.
(16) Bagkar, N.; Widmann, A.; Kahlert, H.; Ravikumar, G.; Yusuf, S. M.; Scholz, F.; Yakhmi, J. V. *Philos. Mag.* **2005**, *85*, 3659.
(17) Chandra, A.; Shukla, M. K.; Mishra, P. C.; Chandra, S. *Phys. Rev. E* **1995**, *51*, R2767.
(18) Besimon, D.; Domany, E.; Aharony, A. *Phys. Rev. Lett.* **1983**, *51*, 1394.
(19) Witten, T. A.; Sunder, L. M. *Phys. Rev. Lett.* **1981**, *47*, 1400.
(20) Peyard, M.; Bishop, A. R. *Phys. Rev. Lett.* **1989**, *62*, 2755.
(21) Glazier, J. A.; Raghavachari, S.; Berthelson, C. L.; Skolnick, M. H. *Phys. Rev. E* **1995**, *51*, 2665.
(22) Sharpe, A. G. *The Chemistry of Cyano Complexes of the Transition Metals*; Academic Press: New York, 1976.
(23) Medina, M. A.; Ramirez, F. J.; Ruiz-Chica, J.; Chavarria, T.; Lopez-Navarrete, J. T.; Sanchez-Jimenez, F. *Biochim. Biophys. Acta* **1998**, *1379*, 129.
(24) Lafuente, C.; Mingotaud, C.; Delhaes, P. *Chem. Phys. Lett.* **1999**, *302*, 523.
(25) Forrest, S. R.; Witten, T. A. *J. Phys. A* **1979**, *12*, L109.
(26) Meakin, P. *Phys. Rev. Lett.* **1983**, *51*, 1119.
(27) Kolb, M.; Botet, R.; Jullien, R. *Phys. Rev. Lett.* **1983**, *51*, 1123.

JP711536R